

# Non-destructive Photo-modulated Reflectance Study of GaInAsSb-based VCSEL

Chai, Grace M T<sup>1</sup>, T. J. C. Hosea<sup>1,2</sup>, N. E. Fox<sup>2</sup>, K. Hild<sup>2</sup>, A. B. Ikyo<sup>2</sup>, I. P. Marko<sup>2</sup>, A. Bachmann<sup>3</sup>, K. Kashani-Shirazi<sup>3</sup>, S. Arafin<sup>3</sup>, M.-C. Amann<sup>3</sup> and S. J. Sweeney<sup>2</sup>

<sup>1</sup>University of Southampton Malaysia, Johor Bahru, 79200, Malaysia

<sup>2</sup>Advanced Technology Institute and Department of Physics, University of Surrey, Guildford, GU2 7XH, UK

<sup>3</sup>Walter Schottky Institut, Technische Universität München, Am Coulombwall 4, D-85748 Garching, Germany  
grace.chai@soton.ac.uk

**Abstract:** Temperature dependent photoreflectance on 2.3μm GaInAsSb -based vertical cavity surface emitting laser (VCSEL) structures were performed and show that the room temperature quantum well-cavity mode energy offset is 21meV; thermally-tuning into resonance at 220±2K. © 2018 The Author(s)  
**OCIS codes:** (300.6380) General; (300.0300)

## 1. Introduction

Realization of efficient lasing in VCSELs is a challenge as it is strongly dependent on the wavelength alignment between the peak of the gain spectrum of the active quantum well (QW) layers and the cavity mode (CM) of the reflectance spectrum of the VCSEL Fabry-Perot structure [1]. A small offset is typically required to account for self-heating above ambient conditions, or for broadening and renormalization effects in the QW gain spectrum. It is useful to be able to monitor the degree of such alignment before full fabrication of the devices. To do that, we performed temperature (T)-dependent photo-modulated reflectance (PR) studies on 2.3μm GaSb-based VCSEL structures prior to device fabrication.

## 2. Samples and Experimental Details

The type I VCSEL GaInAsSb/AlGaAsSb/GaSb wafers, aimed to emit at ~2.33μm at room temperature (RT), were grown by molecular beam epitaxy. They are fully described in reference [2]. To find the alignment at the desired operating temperature between the energy position of the QW ground-state transition ( $E_{QW}$ ) and the CM dip ( $E_{CM}$ ), we used two samples. Sample A is a 2.5cm strip of full VCSEL structure wafer; B is a sample with the top DBR removed. Due to growth conditions the  $E_{CM}$  in sample A varied across the 2.5cm radius of the wafer, blue-shifting by 25nm from the wafer centre to its edge.

RT reflectivity (R) was first undertaken on sample A as a function of incidence angle,  $\theta$ , from 21° to 85° using a single-grating spectrometer, tungsten filament lamp, lock-in amplifier and cooled InSb detector. A mechanical chopper set at 333Hz was placed in front of the spectrometer exit slit so that the light that was to be reflected off the sample was then possible to be detected using lock-in amplification with less background noise. These measured R were then normalised by dividing them by the set-up system response. For the T-dependent PR, the temperature was varied from 9K to 300K at a fixed  $\theta = 45^\circ$ . Both samples were modulated with a 808nm, 450mW GaAlAs diode laser electrically chopped at 812Hz. The samples were mounted in a closed cycle helium cryostat; cooled down to 9K and were heated in suitable steps to measure a sequence of PR spectra up to RT using the same spectrometer, detector and lock-in arrangement described above for the angle-dependent R measurements [3].

## 3. Results and discussion

$E_{CM}$  blue-shifts with the increase of the incident angle,  $\theta$ , of the spectrometer light being shone onto the front surface of the VCSEL structure according to:

$$\lambda_{CM}(\theta) = \lambda_{CM}(0^\circ) \sqrt{1 - \frac{\sin^2(\theta)}{n_{eff}^2}} \quad (1)$$

with  $\lambda_{CM}(0^\circ)$  the normal incidence CM wavelength, and  $n_{eff}$  the refractive index of the effective cavity. The  $\lambda_{CM}(\theta)$  for sample A (not shown here) was fitted with (1) giving  $\lambda_{CM}(0^\circ) = 2.329 \pm 0.001 \mu\text{m}$  and  $n_{eff} = 3.433 \pm 0.003$ . This fit was used later to obtain  $\lambda_{CM}$  at other  $\theta$ . Figs. 1(a) and (b) show the PR spectra from 9K to 325K for samples A and B, respectively. The solid curves are fits with the model in [4]. Both samples' PR show a strong oscillation associated with the CM dip (dashed line,  $E_{CM} = -0.55\text{eV}$  at 9K in sample A).  $E_{CM}$  increases with cooling due to lattice contraction which mainly decreases  $n_{eff}$ , at a rate of  $0.043 \pm 0.002 \text{meV/K}$  for both A and B (see later).  $E_{QW}$  increases with cooling via the band gap energy (but faster than  $E_{CM}$  at  $\sim 29.2 \text{meV/K}$ ). Since  $E_{QW} < E_{CM}$  at RT, then  $E_{QW}$  crosses and comes into resonance with  $E_{CM}$  with increasing temperature [3-5]. Sample A has a higher energy feature (filled

squares) which we interpret as  $E_{QW}$ , but which became unobservable above 125K. In sample B the CM dip results only from the bottom DBR, and is higher ( $\sim 0.57$ eV at 9K) than in sample A. But there are two strong features (filled squares and open circles) due to two QW transitions observable up to 300K. In both samples  $E_{QW} \approx 0.57$ eV at 9K. In sample B,  $E_{QW}$  decreases with increasing T and crosses  $E_{CM}$  at  $\sim 100$ K at  $\sim 0.565$ eV. At 175K, the  $E_{HOT}$  appears at  $\sim 0.57$ eV in sample B (open circles) which also moves and crosses  $E_{CM}$  at  $\sim 250$ K at  $\sim 0.56$ eV.

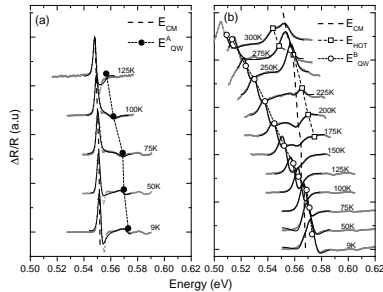


Fig. 1. Detail of normalized T dependent PR spectra for (a) sample A and (b) sample B.

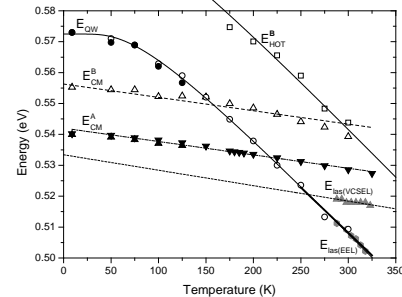


Fig. 2. T-dependence of  $E_{CM}$  (triangles),  $E_{QW}$  (circles) and  $E_{HOT}$  (stars) for samples A (filled symbols) and B (open symbols). Curves are Bose Einstein fits to  $E_{QW}$  &  $E_{HOT}$  [6]. Straight lines are  $E_{CM}$  fit using eq. (1). Grey symbols are edge emitting laser results of [7].

Fig. 2 summarizes the T-dependent results of the measured and fitted energies.  $E_{CM}$  and  $E_{QW}$  for samples A and B agree well. All the  $E_{CM}$  results in Fig. 2 have been shifted to normal incidence values using the linear fit of (1), giving slopes of  $0.043 \pm 0.002$  meV/K in both samples. The circles in Fig. 2 represent the  $E_{QW}$  results: the filled circles are those obtained from fitting the PR spectra of sample A, and the open circles are the corresponding fitted PR results from sample B. These are clearly in good agreement. The curve passing through the  $E_{QW}$  results is a fit with a Bose-Einstein (BE) model [6]. We note that the  $E_{CM}$  results for sample B are  $\sim 15$  meV higher than in sample A. A further study (not discussed here) measuring the RT reflectivity spectra as a function of wafer position across sample A showed that this is caused by two factors: unintended growth variations across both wafers, especially when sample B was taken from the wafer edge; and removal of the sample B top DBR possibly altering the observed  $E_{CM}$  position. The stars in Fig. 2 show the fitted  $E_{HOT}$  PR results for sample B and the curve is the same  $E_{QW}$  BE fit, but shifted up by 35 meV. The fits to the sample A  $E_{CM}$  and  $E_{QW}$  results cross at  $T = 220 \pm 2$  K at energy  $\sim 0.532$  eV. Thus, the PR studies show that the VCSEL will indeed lase at  $\sim 2.3$   $\mu$ m, but the ideal operating T is 220 K. In fact, an ideal VCSEL requires  $E_{QW} > E_{CM}$  at RT, so that they align when the device heats up due to the driving current.

### 3. Conclusions

It has been demonstrated that non-destructive T-dependent PR studies of VCSEL wafers have enabled us to find that the CM occurs at the desired wavelength, 2.3  $\mu$ m. The  $E_{CM}$ - $E_{QW}$  offset is 21 meV at RT. Cooling to  $220 \pm 2$  K makes  $E_{QW} = E_{CM}$  at  $\sim 0.532$  eV ( $\sim 2.33$   $\mu$ m). The utility of the PR VCSEL characterisation technique demonstrates the usefulness of PR for non-destructive pre-fabrication characterization in VCSEL manufacturing. Particularly, it demonstrates the degree of alignment between the QW gain peak and the cavity dip, and the temperature at which they can be brought into resonance, of vital importance for the efficient and successful operation of VCSEL devices.

### 4. References

- [1] P. J. Klar, G. Rowland, T. E. Sale, T. J. C. Hosea, and R. Grey, "Reflectance and Photomodulated Reflectance Studies of Cavity Mode and Excitonic Transitions in an InGaAs/GaAs/AlAs/AlGaAs VCSEL Structure," *Phys. status solidi*, vol. 170, no. 1, pp. 145–158, 1998.
- [2] A. D. L. Cerutti, G. Narcy, P. Grech, G. Boissier, A. Garnache, E. Tournié, F. Genty, "GaSb-based VCSELs emitting in the mid-infrared wavelength range (2–3  $\mu$ m) grown by MBE," *J. Cryst. Growth*, vol. 311, no. 7, pp. 1912–1916, 2009.
- [3] T. J. C. Hosea, "Advances in the application of modulation spectroscopy to vertical cavity structures," *Thin Solid Films*, vol. 450, no. 1, pp. 3–13, 2004.
- [4] S. A. Cripps and T. J. C. Hosea, "An enhanced model for the modulated reflectance spectra of vertical cavity surface emitting laser structures," *Phys. status solidi*, vol. 204, no. 2, pp. 331–342, 2007.
- [5] G. Blume *et al.*, "Cavity mode gain alignment in GaAsSb-based near-infrared vertical cavity lasers studied by spectroscopy and device measurements," *J. Appl. Phys.*, vol. 112, no. 3, pp. 33107–33108, 2012.
- [6] K. P. O'Donnell and X. Chen, "Temperature dependence of semiconductor band gaps," *Appl. Phys. Lett.*, vol. 58, no. 25, pp. 2924–2926, 1991.
- [7] A. B. Ikoye *et al.*, "Gain peak-cavity mode alignment optimisation in buried tunnel junction mid-infrared GaSb vertical cavity surface emitting lasers using hydrostatic pressure," *IET Optoelectron.*, vol. 3, no. 6, pp. 305–309, 2009.